2009 International Symposium on Nonlinear Theory and its Applications
NOLTA'09, Sapporo, Japan, October 18-21, 2009

A New Adaptive Observer for Force-Moment Sensor Calibration

Ying Liu†, Henry Leung ‡, Wallace Kit-Sang Tang †, and Qiang Jia †

†Department of Electronic Engineering, City University of Hong Kong, Tat Chee Avenue, Kowloon, Hong Kong
‡Department of Electrical and Computer Engineering, University of Calgary, Canada
Email: yingliu2@student.cityu.edu.hk, leungh@ucalgary.ca, kstang@ee.cityu.edu.hk, qiangjia@student.cityu.edu.hk

Abstract—In this paper, an adaptive observer is designed to calibrate the force-moment sensor (FMS) of a space robot. Assuming that the mass properties of a payload are known, it is rigourously proved that the calibration matrix can be accurately obtained, based on the measured data from the FMS and the payload displacement recorded by a laser vision system. The effectiveness of the design has also been confirmed with simulation results.

1. Introduction

For the space robotic design, force-moment sensor (FMS) is commonly installed in order to record the forces and the moments caused by the movement of the payload in free space. This information can greatly facilitate the movement of a robot, and hence improve the performance of an assigned motion task. Therefore, the accuracy of the obtained force-moment feedback is very important, and a precise calibration matrix, which converts the sensor reading into the actual forces and moments, is demanded [1, 2].

Traditionally, the calibration matrix is obtained based on the relations between the measurements of the known weight-related loads and their corresponding sensors. In [3], an extended Kalman filter has been employed to perform the sensor calibration of the Special Purpose Dexterous Manipulator (SPDM), based on the movement of a manipulator payload recorded in free space. However, due to the practical issues, this piece of information cannot be accurately inferred from the joint measurement, making this approach less attractive.

To overcome this limitation, the use of high-gain adaptive observer has been suggested in [4]. Two observers, in corresponding to the angular and translational motions of a planar robot, are designed so that its system states and the calibration matrix of its FMS can be estimated. However, this design is relatively complex and a suitable observer gain is to be determined so that the system can be converged. In addition, a slow convergence rate is noticed for the results presented in [4].

In this paper, to further improve the performance on the estimation process of the calibration matrix, a new adaptive observer is suggested. It is found that the body motion and the calibration matrix can be jointly estimated with a faster convergence rate, and it is noise-resistive.

2. Preliminary

Our problem formulation basically follows the suggestions given in [4], and the free-body diagram of the studied planar robot is depicted in Fig. 1. The pose of the robot is described by a rotation angle θ and two orthogonally coordinates X and Y, measured by a laser vision system in an inertial frame J. The force and the moment applied on the payload are then measured by a FMS installed.

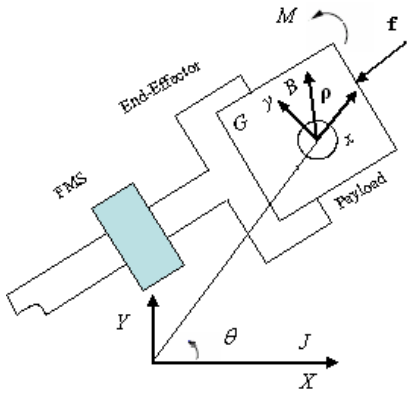

Figure 1: The free-body diagram of a planar robot

It should be noticed that the end-effector and the payload can be jointly treated as an unconstrained rigid body under the action of the resultant force **f** and the moment M applied [4]. Using the Newton-Euler equation [5], it is derived that:

$$\begin{bmatrix} \ddot{\theta} \\ \ddot{X} \\ \ddot{Y} \end{bmatrix} = \frac{1}{m} \begin{bmatrix} m/I_G & -m\rho_y/I_G & m\rho_x/I_G \\ 0 & \cos\theta & -\sin\theta \\ 0 & \sin\theta & \cos\theta \end{bmatrix} \begin{bmatrix} M \\ f_x \\ f_y \end{bmatrix} \tag{1}$$

where θ, X and Y are the displacements of the body in the inertial frame J; m is the mass and I_G is the moment of inertia of the payload about the z-axis passing through the center of mass G. Referring to the body-frame (denoted as B in Fig.1, $\rho = [\rho_x \quad \rho_y]$ is the position vector of the interface of the FMS with the payload, measured from the payload's center of mass; **f** and M are the resultant force and moment applied on the payload, respectively; f_x and f_y are the components of **f**.

Defining the actual wrench as

$$\mathbf{w} = \begin{bmatrix} M & f_x & f_y \end{bmatrix}^T, \tag{2}$$

the measured wrench obtained by FMS, defined as $\hat{\mathbf{w}} = \begin{bmatrix}\hat{M} & \hat{f}_x & \hat{f}_y\end{bmatrix}^T$, will be different from $\mathbf{w}$ due to the sensitivity of the sensor. Their relationship can be described by:

$$\mathbf{w} = \mathbf{S}\hat{\mathbf{w}} \tag{3}$$

where $\mathbf{S} = \{s_{ij}\}$ is a 3×3 calibration matrix.

3. Adaptive Observer Design

3.1. State-space Representation of the Planar Robot

As introduced in [4], the dynamical system (1) can be divided into two subsystems, corresponding to the angular and the translation motions, respectively. Using a state-affine system model [6], the angular motion is then expressed as:

$$\begin{cases} \dot{\mathbf{x}}_1 &= \mathbf{A}_1\mathbf{x}_1 + \mathbf{B}_1(\hat{\mathbf{w}})\varphi_1 \\ \mathbf{y}_1 &= \mathbf{C}_1\mathbf{x}_1 \end{cases} \tag{4}$$

where $\mathbf{x}_1 = [\theta \quad \dot{\theta}]^T$; $\mathbf{C}_1 = [1 \quad 0]$; $\mathbf{A}_1 = \begin{bmatrix} 0 & 1 \\ 0 & 0 \end{bmatrix}$; $\mathbf{B}_1(\hat{\mathbf{w}}) = \frac{1}{I_G}[\mathbf{0}_3 \quad \hat{\mathbf{w}}]^T$; and $\varphi_1 = \begin{bmatrix} s_{11} - \rho_y s_{21} + \rho_x s_{31} \\ s_{12} - \rho_y s_{22} + \rho_x s_{32} \\ s_{13} - \rho_y s_{23} + \rho_x s_{33} \end{bmatrix}$ contains the unknown parameters of the calibration matrix, s_{ij}, as specified in (3).

Similarly, the dynamics of the translation motion are formulated as:

$$\begin{cases} \dot{\mathbf{x}}_2 &= \mathbf{A}_2\mathbf{x}_2 + \mathbf{B}_2(\hat{\mathbf{w}}, \theta)\varphi_2 \\ \mathbf{y}_2 &= \mathbf{C}_2\mathbf{x}_2 \end{cases} \tag{5}$$

where $\mathbf{x}_2 = [X \quad \dot{X} \quad Y \quad \dot{Y}]^T$; $\mathbf{A}_2 = \begin{bmatrix} \mathbf{A}_1 & \mathbf{O}_{2\times2} \\ \mathbf{O}_{2\times2} & \mathbf{A}_1 \end{bmatrix}$; $\varphi_2 = [s_{21}\ s_{22}\ s_{23}\ s_{31}\ s_{32}\ s_{33}]^T$; $\mathbf{C}_2 = \begin{bmatrix} \mathbf{C}_1 & \mathbf{0}_2^T \\ \mathbf{0}_2^T & \mathbf{C}_1 \end{bmatrix}$; $\mathbf{B}_2(\hat{\mathbf{w}}, \theta) = \frac{1}{m}\begin{bmatrix} \mathbf{0}_3 & \hat{\mathbf{w}}\cos\theta & \mathbf{0}_3 & \hat{\mathbf{w}}\sin\theta \\ \mathbf{0}_3 & -\hat{\mathbf{w}}\sin\theta & \mathbf{0}_3 & \hat{\mathbf{w}}\cos\theta \end{bmatrix}^T$; $\mathbf{0}_n$ and $\mathbf{O}_{n\times n}$ denote the n-dimensional zero vector and $n \times n$ zero matrix, respectively.

3.2. Adaptive Observer for State-Parameter Estimation

Referring to the dynamical equations of the angular and the translation motions given in (4) and (5), adaptive observers can be designed as follows:

$$\begin{cases} \dot{\hat{\mathbf{x}}}_1 &= \mathbf{A}_1\hat{\mathbf{x}}_1 + \mathbf{B}_1(\hat{\mathbf{w}})\hat{\varphi}_1 + \mathbf{u}_1 \\ \hat{\mathbf{y}}_1 &= \mathbf{C}_1\hat{\mathbf{x}}_1 \end{cases} \tag{6}$$

and

$$\begin{cases} \dot{\hat{\mathbf{x}}}_2 &= \mathbf{A}_2\hat{\mathbf{x}}_2 + \mathbf{B}_2(\hat{\mathbf{w}}, \theta)\hat{\varphi}_2 + \mathbf{u}_2 \\ \hat{\mathbf{y}}_2 &= \mathbf{C}_2\hat{\mathbf{x}}_2 \end{cases} \tag{7}$$

where $\hat{\mathbf{x}}_1 = [\hat{\theta} \quad \hat{\dot{\theta}}]^T$; $\hat{\mathbf{x}}_2 = [\hat{X} \quad \hat{\dot{X}} \quad \hat{Y} \quad \hat{\dot{Y}}]^T$; $\hat{\varphi}_1$ and $\hat{\varphi}_2$ are the estimators for φ_1 and φ_2, respectively; $\hat{\mathbf{y}}_1$ and $\hat{\mathbf{y}}_2$ are the outputs; $\mathbf{u}_1$ and $\mathbf{u}_2$ are some control signals.

The estimators, $\hat{s}_{ij}$, are adaptively updated by the following rules:

$$\begin{cases} \dot{\hat{s}}_{11} &= \delta\hat{M}e_{\dot{\theta}}/I_G \\ \dot{\hat{s}}_{12} &= \delta\hat{f}_x e_{\dot{\theta}}/I_G \\ \dot{\hat{s}}_{13} &= \delta\hat{f}_y e_{\dot{\theta}}/I_G \\ \dot{\hat{s}}_{21} &= \delta\left[-\hat{M}\rho_y e_{\dot{\theta}}/I_G + \hat{M}e_{\dot{X}}\cos\theta + \hat{M}e_{\dot{Y}}\sin\theta\right] \\ \dot{\hat{s}}_{22} &= \delta\left[-\hat{f}_x\rho_y e_{\dot{\theta}}/I_G + \hat{f}_x e_{\dot{X}}\cos\theta + \hat{f}_x e_{\dot{Y}}\sin\theta\right] \\ \dot{\hat{s}}_{23} &= \delta\left[-\hat{f}_y\rho_y e_{\dot{\theta}}/I_G + \hat{f}_y e_{\dot{X}}\cos\theta + \hat{f}_y e_{\dot{Y}}\sin\theta\right] \\ \dot{\hat{s}}_{31} &= \delta\left[\hat{M}\rho_x e_{\dot{\theta}}/I_G - \hat{M}e_{\dot{X}}\sin\theta + \hat{M}e_{\dot{Y}}\cos\theta\right] \\ \dot{\hat{s}}_{32} &= \delta\left[\hat{f}_x\rho_x e_{\dot{\theta}}/I_G - \hat{f}_x e_{\dot{X}}\sin\theta + \hat{f}_x e_{\dot{Y}}\cos\theta\right] \\ \dot{\hat{s}}_{33} &= \delta\left[\hat{f}_y\rho_x e_{\dot{\theta}}/I_G - \hat{f}_y e_{\dot{X}}\sin\theta + \hat{f}_y e_{\dot{Y}}\cos\theta\right] \end{cases} \tag{8}$$

where $\delta > 0$ is a stiffness constant governing the convergence rates; $e_{\dot{\theta}} = \dot{\theta} - \hat{\dot{\theta}}$, $e_{\dot{X}} = \dot{X} - \hat{\dot{X}}$, $e_{\dot{Y}} = \dot{Y} - \hat{\dot{Y}}$, are the state estimation errors.

The main result of this paper is enunciated in the following theorem:

Theorem 1: Assuming that

1. The system is persistently exciting;
2. Consider a Lyapunov function $V_1(\mathbf{e}_1, \mathbf{e}_2) = \frac{1}{2}\mathbf{e}_1^T\mathbf{e}_1 + \frac{1}{2}\mathbf{e}_2^T\mathbf{e}_2$, where $\mathbf{e}_1 = [e_\theta \quad e_{\dot{\theta}}]^T$, $\mathbf{e}_2 = [e_X \quad e_{\dot{X}} \quad e_Y \quad e_{\dot{Y}}]^T$ denote the angular and translational motion state errors, respectively, there exist controllers $\mathbf{u}_i$, for $i = 1, 2$ such that $\dot{V}_1 < 0$ when φ_i are known;
3. If $\hat{\varphi}_i$ is bounded, i.e. $\|\hat{\varphi}_i\| \le \Phi$, then all the observer's states will be bounded, i.e. $\|\hat{\mathbf{x}}_i\| \le \gamma$, under the control $\mathbf{u}_i$, for $i = 1, 2$, with any initial conditions.

The observer system given (6) and (7) can asymptotically synchronize with the robotic system (4) and (5), while simultaneously, $\hat{s}_{ij}$ converge to their true values, s_{ij}. In other word, $\hat{\mathbf{x}} \to \mathbf{x}$ and $\hat{\mathbf{S}} \to \mathbf{S}$ as $t \to \infty$.

Proof: Subtracting (6) from (4), the error dynamics of the angular model are obtained as:

$$\dot{\mathbf{e}}_1 = \mathbf{A}_1\mathbf{e}_1 - \mathbf{u}_1 + \mathbf{B}_1(\hat{\mathbf{w}})\Delta\varphi_1 \tag{9}$$

Similarly, subtracting (7) from (5), the error dynamics of translational model can be expressed as:

$$\dot{\mathbf{e}}_2 = \mathbf{A}_2\mathbf{e}_2 - \mathbf{u}_2 + \mathbf{B}_2(\hat{\mathbf{w}})\Delta\varphi_2 \tag{10}$$

where $\Delta\varphi_i = \varphi_i - \hat{\varphi}_i$ for $i = 1, 2$.

Consider the following Lyapunov function:

$$V = \frac{1}{2}\mathbf{e}_1^T\mathbf{e}_1 + \frac{1}{2}\mathbf{e}_2^T\mathbf{e}_2 + \sum_{i=1}^{3}\sum_{j=1}^{3}\frac{1}{2\delta}\Delta s_{ij}^2 \tag{11}$$

where $\Delta s_{ij} = s_{ij} - \hat{s}_{ij}$, and differentiate (11), one has

$$\dot{V} = \frac{1}{2}\dot{\mathbf{e}}_1^T\mathbf{e}_1 + \frac{1}{2}\mathbf{e}_1^T\dot{\mathbf{e}}_1^T + \frac{1}{2}\dot{\mathbf{e}}_2^T\mathbf{e}_2 + \frac{1}{2}\mathbf{e}_2^T\dot{\mathbf{e}}_2^T - \sum_{i=1}^{3}\sum_{j=1}^{3}\frac{1}{\delta}\Delta s_{ij}\dot{\hat{s}}_{ij}$$

$$
\begin{aligned}
&= \frac{1}{2}(\mathbf{A}_1\mathbf{e}_1 - \mathbf{u}_1)^T\mathbf{e}_1 + \frac{1}{2}\mathbf{e}_1{}^T(\mathbf{A}_1\mathbf{e}_1 - \mathbf{u}_1) \\
&\quad + \mathbf{e}_1{}^T(\mathbf{B}_1(\hat{\mathbf{w}})\Delta\varphi_1) + \frac{1}{2}(\mathbf{A}_2\mathbf{e}_2 - \mathbf{u}_2)^T\mathbf{e}_2 \\
&\quad + \frac{1}{2}\mathbf{e}_2{}^T(\mathbf{A}_2\mathbf{e}_2 - \mathbf{u}_2) + \mathbf{e}_2{}^T(\mathbf{B}_2(\hat{\mathbf{w}}, \theta)\Delta\varphi_2) \\
&\quad - \mathbf{e}_1{}^T(\mathbf{B}_1(\hat{\mathbf{w}})\Delta\varphi_1) - \mathbf{e}_2{}^T(\mathbf{B}_2(\hat{\mathbf{w}}, \theta)\Delta\varphi_2) \\
&= \frac{1}{2}(\mathbf{A}_1\mathbf{e}_1 - \mathbf{u}_1)^T\mathbf{e}_1 + \frac{1}{2}\mathbf{e}_1{}^T(\mathbf{A}_1\mathbf{e}_1 - \mathbf{u}_1) \\
&\quad + \frac{1}{2}(\mathbf{A}_2\mathbf{e}_2 - \mathbf{u}_2)^T\mathbf{e}_2 + \frac{1}{2}\mathbf{e}_2{}^T(\mathbf{A}_2\mathbf{e}_2 - \mathbf{u}_2) \\
&= \dot{V}_1 \qquad (12)
\end{aligned}
$$

with the assumption (2), $V = \dot{V}_1 \leq 0$ and hence, the state estimation errors converge to zero when $t \to \infty$. Based on assumption (1) and the Barbalat's theorem [7], $\Delta s_{ij} \to 0$, i.e. $\hat{s}_{ij} \to s_{ij}$ as $t \to \infty$, and that completes the proof.

Remark 1: In a practical case, the time derivative functions, $\dot{\theta}$, $\dot{X}$ and $\dot{Y}$, may not be observable, and hence $e_{\dot{\theta}}$, $e_{\dot{X}}$ and $e_{\dot{Y}}$ are unknown. However, they can be approximated by backward difference equation, using θ, X and Y.

4. Numerical Simulations

A number of simulations have been carried out to illustrate the effectiveness of the proposed design. In order to compare the performance with the high gain adaptive observer, the same settings which have been used in [4] are adopted:

1. The payload of the mass is 2.50 kg;
2. The moment of inertia is 0.75 kgm^2 attached to the end-effector of a planar manipulator through a FMS, located at $\rho = [0.2 \quad 0.25]^T$ meters from the center of mass of the payload in B frame;
3. The kinematics of the payload are expressed as:

$$
\begin{cases}
M = \sin(2t) + 0.1\cos(10t) + 0.4\sin(\pi t + \pi/6) \\
f_x = \sin(t) + 0.1\cos(4.5t) + 0.4\sin(\pi t + \pi/3) \\
f_y = 2\sin(3t) + 0.2\cos(5t) + 0.4\sin(7t)
\end{cases} \qquad (13)
$$

4. The actual calibration matrix is assumed to be:

$$
\mathbf{S} = \begin{bmatrix} 0.6110 & -0.0372 & -0.1445 \\ -0.3361 & 1.0020 & -0.1443 \\ -0.1147 & 0.1674 & 0.9598 \end{bmatrix}.
$$

Remark 2: The kinematics given in (13) provide the persistently excitation for the system.

Referring to (6) and (7), a linear output feedback is used as the control signal $\mathbf{u}_i$, which is given as:

$$
\mathbf{u}_i = \mathbf{K}_i(\mathbf{y}_i - \hat{\mathbf{y}}_i) = \mathbf{K}_i\mathbf{C}_i\mathbf{e}_i \quad \text{for} \quad i = 1, 2 \qquad (14)
$$

where $\mathbf{K}_1 = [25 \quad 25]^T$ and $\mathbf{K}_2 = \begin{bmatrix} 5 & 10 & 2 & 5 \\ 5 & 5 & 15 & 15 \end{bmatrix}^T$.

Referring to Remark 1, $e_{\dot{\theta}}$, $e_{\dot{X}}$ and $e_{\dot{Y}}$ in (8) may not be available. In our simulation, backward difference approximation is used, for example,

$$
\begin{aligned}
e_{\dot{\theta}}(n) &= \dot{\theta}(n) - \hat{\dot{\theta}}(n) \\
&\simeq [\theta(n) - \theta(n-1)] - [\hat{\theta}(n) - \hat{\theta}(n-1)] \qquad (15) \\
&\simeq e_\theta(n) - e_\theta(n-1)
\end{aligned}
$$

The time interval is omitted in (15) as it is absorbed in the stiffness constant δ, which is set to be 20 in our case. Similar expressions are obtained for $e_{\dot{X}}$ and $e_{\dot{Y}}$.

The vector $\hat{\mathbf{w}}$ in (6) and (7) is obtained by taking the inverse of (3), i.e. $\hat{\mathbf{w}} = \hat{\mathbf{S}}^{-1}\mathbf{w}$, where the measured payload forward dynamics are needed. Recognizing that measurement and/or environmental noises are inevitably existed, a Gaussian noise with zero mean and variance of 5% of the amplitude to each element is added to the wrench data in simulations. Similarly, Gaussian noise is injected to the angular and translational-displacement measurements, with zero mean and variances of 0.1° and 0.1mm, respectively.

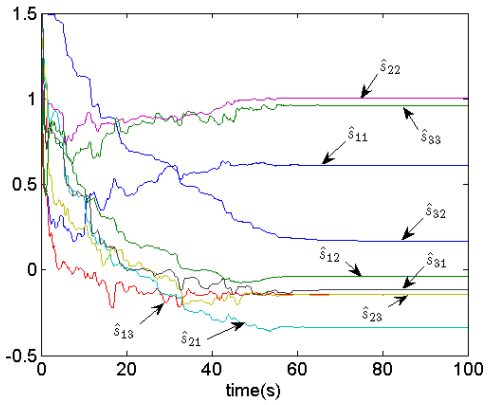

Figure 2: The estimators $\hat{s}_{ij}$ for s_{ij} against time

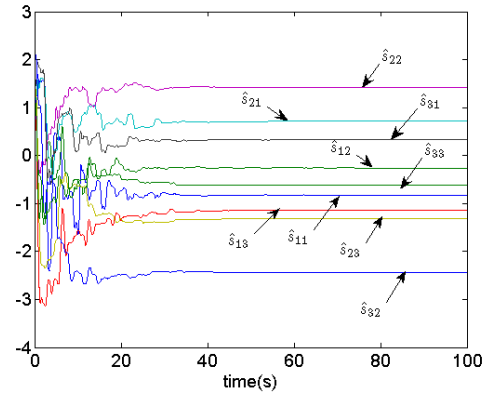

Figure 3: The estimators $\hat{s}_{ij}$ for s_{ij} against time

Figure 2 depicts the values of $\hat{s}_{ij}$ obtained for a simulation period of 100 seconds. The integration step size is set to be 1ms and the initial guesses of $\hat{s}_{ij}$ are randomly selected between [0, 3].

Table 1: The values of s_{11}, s_{22}, s_{33} in 0-300s

	[0 100)	[100 200)	[200 300]
s_{11}	0.6110	0.3847	-0.2839
s_{22}	1.0020	0.8144	0.5472
s_{33}	0.9598	0.9169	1.1172

It can be observed that $\hat{s}_{ij}$ converge to their corresponding true values very quickly, and a transient time of about 70s is noticed. Taking the result at 100s, we have:

$$\hat{\mathbf{S}} = \begin{bmatrix} 0.6105 & -0.0366 & -0.1445 \\ -0.3358 & 1.0017 & -0.1443 \\ -0.1148 & 0.1676 & 0.9597 \end{bmatrix}.$$

In order to evaluate the accuracy of the obtained results, the induced 2-norm of estimation error proposed in [8] is used, which is expressed as:

$$E = \|\mathbf{I} - \hat{\mathbf{S}}\mathbf{S}^{-1}\| \tag{16}$$

where $\mathbf{I}$ is an identity matrix.

Based on the proposed observer design, $E = 9.1106 \times 10^{-4}$ after 100s, which is much smaller than $E = 3.6700 \times 10^{-2}$ when the high-gain observer [4] is used. Moreover, it is also noticed that a faster convergence rate is achieved based on our design.

A more noisy case is also investigated and the results are shown in Fig. 3. The variance of the Gaussian noise is increased to about 10% of the amplitude to each wrench element while the variances of the angular and translational-displacement measurements are augmented to be 1° and 0.2 m, respectively. Moreover, the entities of the calibration matrix are randomly selected within [-3, 3]. From Fig. 3, it can be observed that a similar performance is achieved, and hence it is concluded that the design is noise-resistive.

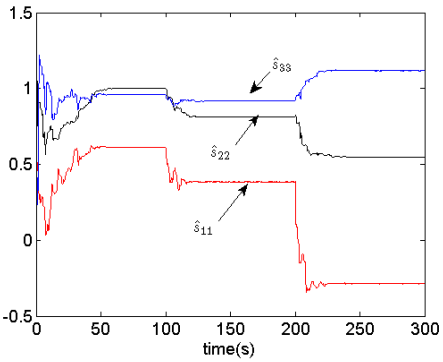

Figure 4: The estimators $\hat{s}_{ij}$ for s_{ij} against time

Since the properties of FMS may change gradually, simulation with time-varying calibration matrix is also performed. Assuming that the entities, s_{11}, s_{22}, s_{33}, change with time according to the values specified in Table 1, the simulation results are shown in Fig.4. Clearly, these slow variations are duly captured and true values of s_{11}, s_{22}, s_{33} are obtained. However, it should be remarked that it becomes incompetent if the variation changes too fast.

5. Conclusions

In this paper, a novel adaptive observer has been proposed to calibrate the FMS of a planar robotic system. By measuring the payload displacement with a laser vision system, a calibration matrix for the FMS can be accurately determined. The effectiveness of the design has been mathematically proved with the Lyapunov stability theorem, and illustrated by numerical simulations. In addition, noisy condition and time-varying situation are also considered, and satisfactory results are reported. As compared with the design presented in [4], this new adaptive observer is simpler in nature and a faster convergence rate is experienced.

Acknowledgments

This work is fully supported by grants from the Research Grants Council of Hong Kong Special Administrative Region, China, CityU 120407 and 120708.

References

[1] M. M. Sivinin, and M. Uchiyama, "Optimal geometric structures of force/torque sensors," *Int. J. Robotics Research*, vol.14, pp.560-573, 1995.

[2] P. C. Hughes, "Space structure vibration modes: How many exist? which ones are important?" *IEEE Control Magazine*, vol.7, no. 1, pp. 22C28, February 1987.

[3] F. Aghili, "On-orbit calibration of the SPDM force-moment sensor," *in Proc. IEEE Int. Conf. Robotics and Automation, Francisco*, CA, April 2000.

[4] K. Parsa and F. Aghili, "Adaptive Observer for the Calibration of the Force-Moment Sensor of a Space Robot," *Proceedings of the 2006 IEEE International Conference on Robotics and Automation Orlando, Florida*, May 2006.

[5] H. Goldstein, *Classical Mechanics*, 2nd ed. Reading, MA: Addison-Wesley, 1980.

[6] J. P. Gauthier, H. Hammouri, and S. Othman, "A simple observer for nonlinear systems: Applications to bioreactors," *IEEE Trans. Automatic Control*, vol. 31, no. 6, pp. 875C880, 1992.

[7] H. K. Khalil, *Nonlinear Systems*, Upper Saddle River, N.J.: Prentice Hall, c2002.

[8] R. A. Horn and C. R. Johnson, *Matrix Analysis*, Cambridge, England: Cambridge University Press, 1990.